Optical design for Antarctic Bright Star Survey Telescope

Zhengyang Li (李正阳)[1,2,*], Haipin Lu (卢海平)[1,2], and Xiangyan Yuan (袁祥岩)[1,2]

[1]*National Astronomical Observatories/Nanjing Institute of Astronomical Optics and Technology, Chinese Academy of Sciences, Nanjing 210042, China*

[2]*Key Laboratory of Astronomical Optics & Technology, Nanjing Institute of Astronomical Optics and Technology, Chinese Academy of Sciences, Nanjing 210042, China*

**Corresponding author: zyli@niaot.ac.cn*

Received June 24, 2015; accepted September 18, 2015; posted online October 14, 2015

The exoplanet search is one of the most exciting research fields in astrophysics. The Antarctic Bright Star Survey Telescope (BSST), capable of continuous exoplanet observation on polar nights, is a Ritchey–Chretien telescope with a three-lens field corrector, and has a 300 mm aperture, 2.76 focal ratio, and a wavelength coverage ranging from 0.36 to 1.014 μm. Equipped with a 4 k × 4 k and 12 μm/pixel CCD camera, the BSST can gain a field of view of 4.8°. This Letter presents the optical design, tolerance analysis, and the alignment plan for the BSST, and the test observation results.

OCIS codes: 110.0110, 220.0220, 230.0230.
doi: 10.3788/COL201513.111101.

Astronomers need advanced telescopes and qualified observation sites to observe the far and faint stars. The Antarctica plateau is widely considered to be an excellent astronomical site due to its superb seeing conditions[1]. On polar nights, the *in situ* Antarctic telescopes manage to continuously observe the sky for three months, which is quite suitable for transit detection and time-domain astronomy.

Several Chinese wide-field Antarctic telescopes have been built. The first generation was the Chinese Small Telescope Array (CSTAR), which is composed of four identical telescopes with a 145 mm entrance pupil and a 20 square degrees field of view (FOV). CSTAR is fixed to point at the South Pole, and is mainly used for variable star detection and atmosphere extinction measurements. It was deployed in Antarctica in 2008 and its automatic operation continued for four consecutive winters[2]. The second generation was the three Antarctic Survey Telescopes (AST3), each with a 500 mm entrance pupil and an 8.5 square degrees FOV. AST3-1 and AST3-2 were respectively mounted on the Antarctic plateau in 2012 and 2015, for supernovae survey and to search for exoplanets[3].

The Antarctic Bright Star Survey Telescope (BSST), which mainly looks for exoplanets by searching with transit detection with a photometric precision of less than 0.6% magnitude, has a 300 mm aperture, an f-ratio of 2.76, and a FOV of 4.8° (3.4 × 3.4°). It has seven filters (one open band, three wide-band filters of the B, V, R bands, and three narrow-band filters of H–α, H–β, and O–3 bands), all of which allow for a wavelength coverage from 0.36 to 1.01 μm. A 4 k × 4 k and 12 μm/pixel CCD camera from Andor Technology is used for imaging of the 3 arcsec/pixel. The optical performance for the central 30 arcmin FOV requires 80% energy encircled within 2 pixels, and for the whole FOV, 80% energy encircled within 5 pixels. In particular, the BSST requires qualified operation at both the domestic sites and Antarctic sites. The telescope will be installed at Antarctic Zhongshan Station in January 2016.

There are several well-known optical systems for wide-field astronomical telescopes. The optical systems are the catadioptrics, such as CSTAR; the Schmidt and quasi-Schmidt types, such as AST3, and the Large Sky Area Multi-Object Fibre Spectroscopic Telescope (LAMOST). There are also the R–C two-mirror reflectors with correctors, such as the Visible and Infrared Survey Telescope for Astronomy (VISTA)[4], and the three-mirror systems, such as the Large Synoptic Survey Telescope (LSST) and the proposed Kunlun Dark Universe Survey Telescope (KDUST)[5,6].

The optics for CSTAR, AST3, and KDUST are not suitable for the BSST, since CSTAR has a larger light obstruction and a small back focal length with a fixed focal plane. AST3 is equipped with a camera located inside the optical tube, which is not convenient for installation or maintenance; the three-mirror systems are mainly for large telescopes with high resolutions. Considering the large dimension of selected CCD camera and the multi-band filters switching mechanism, we decided to design an R–C telescope with a larger back focal length for the BSST.

The optical layout of an R–C telescope is illustrated in Fig. 1[7]. When calculating the initial parameters of the optical system, the following decisions must be made:

1. Generally, an R–C telescope's optical performance is free of a coma aberration and dominated by astigmatic aberration. And the astigmatism will increase by reducing the primary mirror focal ratio (F number). On the other hand, it is easier to align a telescope with a primary mirror with a larger F. Therefore, we decided to use a primary mirror with a 1.3F number, and a focal length f_1' of 400 mm.

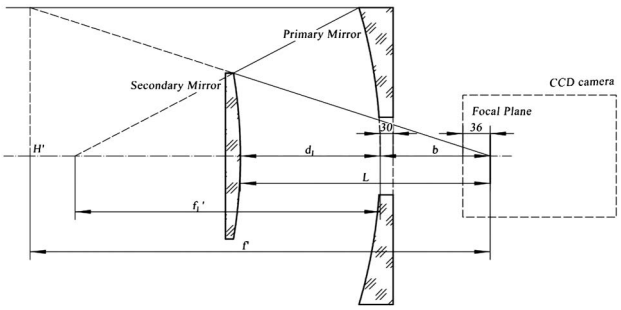

Fig. 1. Schematic drawing of R–C telescope.

2. Mechanical devices for filter switching and focusing demand a larger back focal length. A suitable value of back focal length b must guarantee a 30 mm thickness of the primary mirror, and an extra 36.5 mm for the inside CCD chip, and a margin for the filter wheel mechanism. Thus, we used $b = 130$ mm.
3. The CCD pixel size is 12 μm and its imaging scale is 3 arcsec/pixel; hence, the system's focal length f' is 825 mm. The magnification of the secondary mirror m_2 is −2.06.

Referring to "Reflective Telescope Optics," an axial obstruction ratio R_A can be written as[8]

$$R_A = \frac{L}{f'} = \frac{d_1 + b}{f'}. \tag{1}$$

Then, f' and f_2' are given by

$$f' = \frac{d_1 m_2}{1 - R_A}, \tag{2}$$

$$f_2' = \frac{R_A f' L}{L + R_A f_1'}. \tag{3}$$

The conic coefficients of the primary and secondary mirrors can be deduced based on the calculation of the Seidel aberrations coefficients, as

$$b_p = -1 - \frac{2L}{d_1 m_2^3}, \tag{4}$$

$$b_s = -\left[\left(\frac{m_2 - 1}{m_2 + 1}\right)^2 + \frac{2f'}{d_1(m_2 + 1)^3}\right]. \tag{5}$$

As $f' = 825$ mm, $f_1' = -400$ mm, $m_2 = -2.06$, and $b = 130$ mm, based on Eqs. (1)–(5), the major parameters can be calculated as shown in Table 1.

Then, we used the ZEMAX software for thorough optimization. Finally, an R–C telescope system with a three-lens corrector was obtained, which delivered a qualified performance for the wide field and the multiband system. The optical parameters are listed in Table 2.

There are two critical problems for the special Antarctic telescopes, which will be operated at a temperature ranging from −80°C to 40°C. Firstly, the mirrors will frost when the ambient atmosphere warms up quickly or dramatically in Antarctica. Secondly, the optical performances will degrade as a result of the temperature deformation.

Table 1. Initial Optical Configuration of BSST

Optical Element	Radius (mm)	Conic Coefficient	Distance (mm)
Primary Mirror	−800	−1.33	227.1
Secondary Mirror	−639.9	−14.16	357.1

Considering the dilemmas, we used a defrost window with an indium-tin-oxide film coating to seal the tube, which will be filled with nitrogen. The window's frontier surface can be heated to protect the window from frosting up. Additionally, we selected a low-thermal-expansion optical material, such as Zerodur or fused silica glass, to minimize the thermal effect. However, we had to use a TF3 material for to correct the chromatic aberration.

For the open-band (0.36–1.014 μm) configuration shown in Fig. 2, the distance between the corrector and the insulated window is 40 mm, and a 7 mm-thick filter can be fitted in. The filters, listed in Table 3, were purchased from the Andover Corporation. The apertures of the filters are 50 mm for the wide bands and 25 mm for the narrow bands, which is a value that is smaller than 80 mm of the open band. The clear FOV, without vignetting for B, V, R is about 3°, and 25 arcmin for the narrow bands, which can satisfy the demands for special targeted observations.

For the open-band configuration, the optical performances are illustrated by Figs. 3 and 4. The diameter of 80% encircled energy is 31.6 μm for a 4.8° FOV, and 15.6 μm for a 30 arcmin FOV. The image quality of the entire field is superior to 3 pixels, which meets the requirements and can tolerate the manufacturing process and assembly.

By using at least three different materials, an apochromatic system can possibly be achieved with less coma and

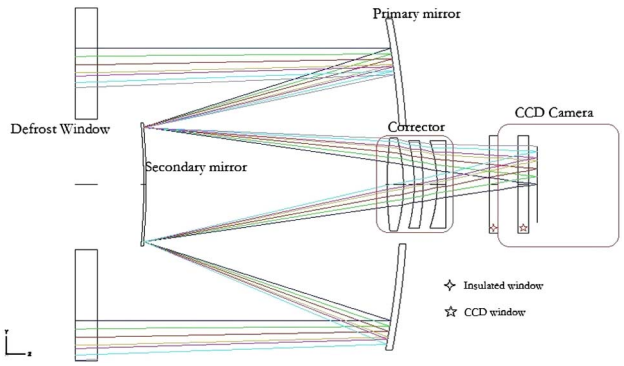

Fig. 2. BSST optical layout of open-band configuration. (The filter is located before the insulated window).

Table 2. Optical Configuration of BSST

Optical Element	Radius (mm)	Conic Coefficient	Thickness (mm)	Diameter (mm)	Glass
Defrost Window	Infinity	–	20	324	Fused silica
	Infinity	–	280		
Primary Mirror	−800	−1.519	235	315	Zerodur
Secondary Mirror	−606	−14.443	222	113	Zerodur
Lens 1	358	–	15	90	Fused silica
	−159.9	–	10		
Lens 2	−159.9	–	8	84	TF3
	−239.66	–	13		
Lens 3	−123.59	–	8	80	Fused silica
	Infinity	–	40		
Insulated Window	Infinity	–	8	90	Fused silica
	Infinity	–	18.5		
CCD Window	Infinity	–	9.5	90	Fused silica
	Infinity	–	8		
Focal Plane	Infinity	–		70	–

Table 3. Parameters of Filters

Filter	Central Wavelength (nm)	Bandwidth (nm)	Transmission (%)	Diameter (mm)
B	440	100	>50	50
V	550	90	>70	50
R	760	250	>70	50
H–α	656.3	10	>50	25
H–β	486.1	10	>40	25
O–3	500.7	10	>60	25

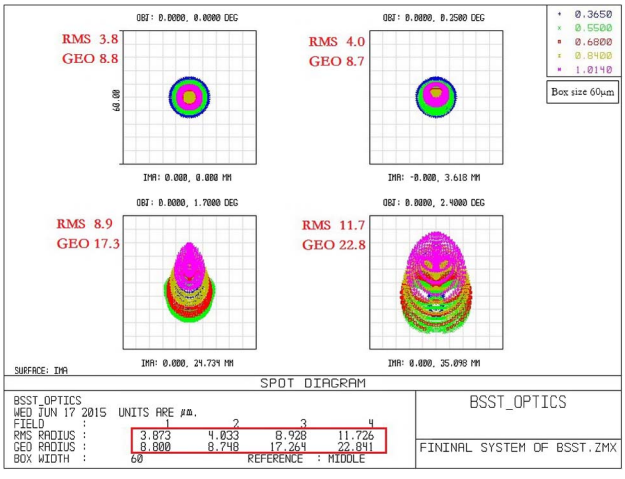

Fig. 3. Image spot diagram of BSST (the box is 60 μm).

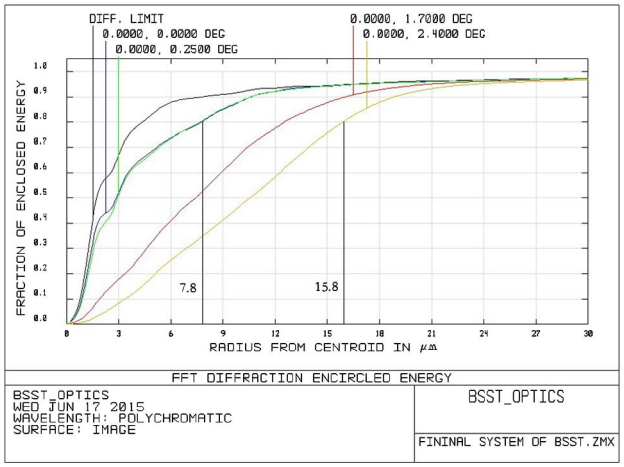

Fig. 4. Diffraction-encircled energy layout.

chromatism aberrations[9]. However, it will multiply the difficulties of the thermal control system. From an economical perspective, the proposed BBST optics is the optimal and simplest option.

When we finished with the design, an error budget analysis helped us to build a reasonably priced system. During the tolerance analysis procedure, we defined a focal compensator, and used the Monte–Carlo simulation to predict the statistical effects by simulating more than 300 random systems that meet all of the tolerance values, which are listed in Table 4. The resulting 80% encircled energy diameters of the fields (0.5°, 1.7°, and 2.4°) were then recorded and are shown in Fig. 5. Of the set of given tolerance values, the optical performances can be

Table 4. Tolerance Values of BSST

Manufactory Error Budget				
Items	Thickness (mm)	Radius (mm)	Conic	Nominal
Primary	–	±1 mm	±0.0001	(−800; −1.519)
Secondary	–	±1 mm	±0.0001	(−606; −14.443)
Lens	−0.1	–	0	(15, 8, 8)
Alignment Error Budget				
DOF	Decenter (mm)		Tilt	Position (mm)
Primary	DATUM			
Secondary	±0.06		±1′	±0.4
Corrector	±0.1		±3.6′	±0.4
Lens Space	–		–	±0.1
Use Focal Length as Compensator				

described as follows: in 90% of the possibilities, there will be 80% energy encircled within 5.7 arcsec in the central FOV, and 11.9 arcsec in the edge FOV. It predicts that the BSST image quality will surpass the requirement (80% energy of the entire FOV encircled within 5 pixels). The tolerance analysis ensures that the BSST manufacturing process and alignment are both feasible.

When assembling the BSST in the laboratory, we can predict the misalignment states with the aberration measurements. The optical performance of a misaligned R–C telescope can be described as resulting in field-dependent astigmatism and a field-uniform coma[10]. Typically, there is always a point on a two-mirror telescope's optical axis at which the translation coma resulting from the decentering and the rotation coma resulting from the tilt will cancel out. This is known as the coma-free point (CFP)[8]. The residual aberrations of the BSST are shown in Fig. 6, where the secondary mirror tilted around the CFP can be seen. The misaligned aberrations are illustrated in Fig. 7, and Fig. 8 demonstrates the misaligned aberration maps resulting from the secondary mirror decentering.

The field behaviors of the astigmatism and coma indicate that we can minimize the astigmatism by secondary tilting and lower the chance of a coma by secondary translating separately[11]. Combined with a four-dimensional interferometer, we managed to aligned the BSST's

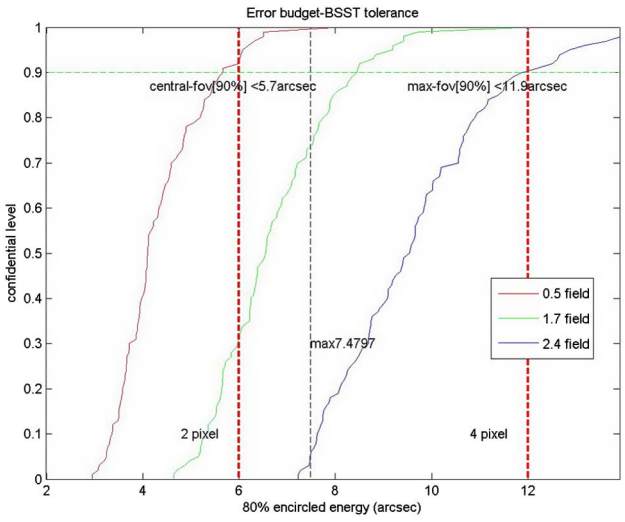

Fig. 5. Resulting 80% encircled energy diameters.

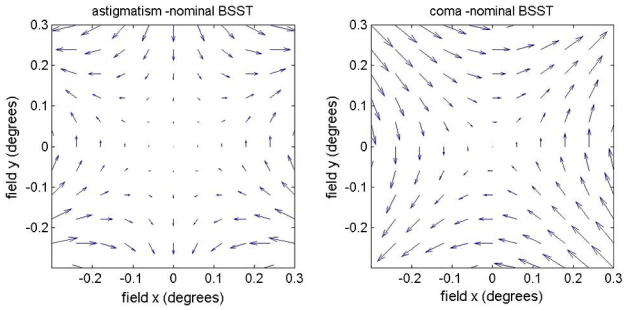

Fig. 6. Residual astigmatism and coma field behavior (the arrows on the maps show the amplitude and direction of the aberrations sampling from various fields).

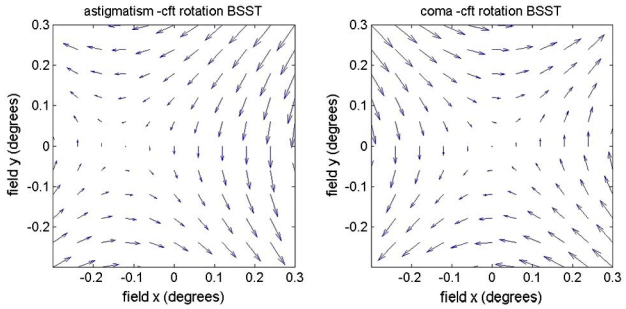

Fig. 7. Astigmatism and coma field behavior of tilting secondary mirror around the CFP.

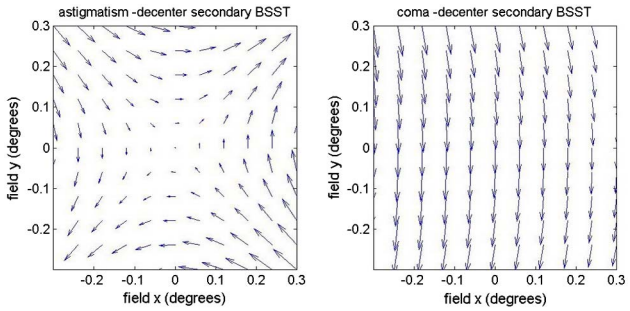

Fig. 8. Astigmatism and coma field behavior of translating secondary mirror.

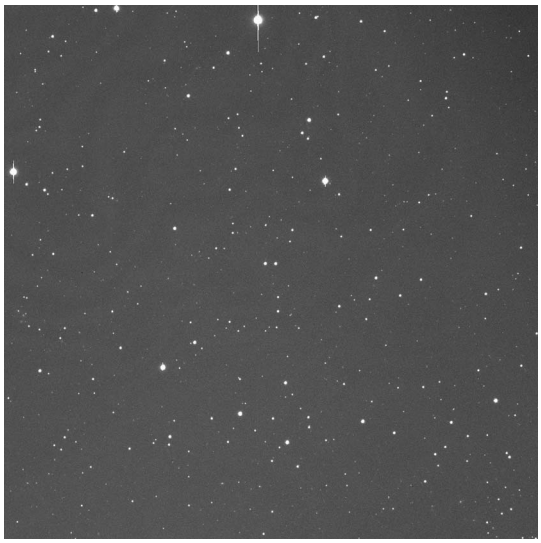

Fig. 9. BSST image of 120 s exposure in the R band (1200 pixels × 1200 pixels).

secondary mirror. The metrology is accurate, but time consuming. A more valuable metrology is under study by calculating the distribution of a star image's ellipticity.

In April 2015, the telescope completed its test observation at Gaomeigu station (Yunnan Observatory) before we transported the BSST to Zhongshan Station in Antarctica. Figure 9 shows a star image of 120 s exposure in the R band. The photometric results of Fig. 9 show that the BSST is able to image a target with a magnitude of 17.1 with a signal-to-noise ratio value of 20. Moreover, the median FWHM value is 1.7 pixels of the central FOV and less than 2.6 pixels of the entire FOV. The photometric precision is superior to a magnitude of 0.4%, which was measured in the transit detection and will be discussed in another Letter.

The Antarctic telescopes are special, and the experiences of the CSTAR and AST3 projects provide us with many things to consider when designing and building the BSST. This Letter presents the optical system design, tolerance analysis, and alignment metrology of the unique and powerful Antarctic BBST. Eventually, the test observation results indicate that the BSST is a superior telescope with a 4.8° FOV and 0.36–1.014 μm wavelength coverage. The BSST is capable of delivering a qualified performance with a limiting magnitude of at least 17 m and a photometric precision of 0.4% m, which should convince astronomers of its ability to make significant discoveries in the search for exoplanets when it is deployed in Antarctica.

The authors would like to thank Polar Research Institute of China and the University of Science and Technology of China for their support and cooperation. We appreciate the assistance of the Yunnan Observatory for the BSST test observation. The work was supported by the SOC program (CHINARE2012-02-03).

References

1. J. S. Lawrence, M. C. B. Ashley, A. Tokovinin, and T. Travouillon, Nature **431**, 278 (2004).
2. G. Liu and X. Yuan, Acta Astron. Sin. **50**, 224 (2009).
3. X. Yuan and D. Su, MNRAS **424**, 23 (2012).
4. W. Sutherland, J. Emerson, G. Dalton, E. Atadettedgui, S. Beard, R. Bennett, N. Bezawada, A. Born, M. Caldwell, P. Clark, S. Craig, D. Henry, P. Jeffers, B. Little, A. McPherson, J. Murray, M. Stewart, B. Stobie, D. Terrett, K. Ward, M. Whalley, and G. Woodhouse, A&A **575**, A25 (2015).
5. C. F. Claver, L. Seppala, M. Liang, K. Gilmore, W. Gressler, V. Krabbendam, D. Niell, S. Oliver, and J. Sebag, "Performance and Analysis of the LSST Optical System," http://www.lsst.org/sites/default/files/docs/137.18_Claver_Optical_System_8x10.pdf (2010).
6. X. Yuan, X. Cui, D. Su, Y. Zhu, L. Wang, B. Gu, X. Gong, and X. Li, Proc. Int. Astron. Union. **8**, 271 (2013).
7. X. Hu, W. Wang, Q. Hu, X. Lei, Q. Wei, Y. Liu, and J. Wang, Chin. Opt. Lett. **12**, 072901 (2014).
8. R. Wilson, *Reflecting Telescope Optics I* (Springer, 2004).
9. Q. Yang, B. Zhao, and R. Zhou, Chin. Opt. Lett. **6**, 146 (2008).
10. K. Thompson, J. Opt. Soc. Am A **22**, 1389 (2005).
11. Z. Li and X. Yuan, Proc. SPIE **9150**, 91501Y (2014).